Chemotaxis toward phytoplankton drives organic matter partitioning among marine bacteria

Steven Smriga[a,b,1], Vicente I. Fernandez[a,b,1], James G. Mitchell[c,d], and Roman Stocker[a,b,2]

[a]Ralph M. Parsons Laboratory, Department of Civil and Environmental Engineering, Massachusetts Institute of Technology, Cambridge, MA 02139; [b]Department of Civil, Environmental and Geomatic Engineering, ETH Zurich, 8092 Zurich, Switzerland; [c]School of Biological Sciences, Flinders University, Adelaide, SA 5001, Australia; and [d]Flinders Centre for Nanoscale Science and Technology, Flinders University, Adelaide, SA 5001, Australia

Edited by Tom M. Fenchel, University of Copenhagen, Helsingor, Denmark, and approved December 15, 2015 (received for review June 25, 2015)

The microenvironment surrounding individual phytoplankton cells is often rich in dissolved organic matter (DOM), which can attract bacteria by chemotaxis. These "phycospheres" may be prominent sources of resource heterogeneity in the ocean, affecting the growth of bacterial populations and the fate of DOM. However, these effects remain poorly quantified due to a lack of quantitative ecological frameworks. Here, we used video microscopy to dissect with unprecedented resolution the chemotactic accumulation of marine bacteria around individual *Chaetoceros affinis* diatoms undergoing lysis. The observed spatiotemporal distribution of bacteria was used in a resource utilization model to map the conditions under which competition between different bacterial groups favors chemotaxis. The model predicts that chemotactic, copiotrophic populations outcompete nonmotile, oligotrophic populations during diatom blooms and bloom collapse conditions, resulting in an increase in the ratio of motile to nonmotile cells and in the succession of populations. Partitioning of DOM between the two populations is strongly dependent on the overall concentration of bacteria and the diffusivity of different DOM substances, and within each population, the growth benefit from phycospheres is experienced by only a small fraction of cells. By informing a DOM utilization model with highly resolved behavioral data, the hybrid approach used here represents a new path toward the elusive goal of predicting the consequences of microscale interactions in the ocean.

bacteria–phytoplankton interactions | motility | competition | microbial loop | dissolved organic matter

Bacteria in the ocean compete for organic matter to support growth. Strategies for the acquisition of organic matter span a continuum whose extremes are oligotrophy and copiotrophy (1–3). Oligotrophic taxa thrive in low-nutrient conditions and dominate bacterial assemblages in most oceanic provinces, whereas copiotrophs are adapted for growth in resource-rich conditions, such as coastal phytoplankton blooms (4), and can account for much of the carbon uptake by a microbial assemblage (5). However, the growth advantages of coexisting populations of marine bacteria with different adaptations, in relation to realistic resource landscapes, is challenging to study and frequently neglected in microbial oceanography, reflecting the need for a quantitative ecological framework for the foraging of marine microorganisms and its ecosystem consequences (6).

One adaptation frequently differentiating copiotrophs from oligotrophs is motility (2), which typically entails chemotaxis, the ability to sense and move toward a chemical source. Phytoplankton and detrital particles exude dissolved organic matter (DOM), creating strong localized hotspots that fall off through steep gradients into background levels of DOM in bulk seawater (7). For phytoplankton, this microenvironment is called the "phycosphere" (8) and its composition will vary for healthy, stressed, or dead phytoplankton. Chemotaxis allows some copiotrophic bacteria to accumulate in resource-rich locations and significantly increase their exposure to DOM in transient microscale hotspots (9–13). However, the long-term value of chemotaxis for populations may depend on environmental conditions, because the prevalence of motile cells varies widely in natural communities (14, 15), and genes associated with chemotaxis can be sparse in typical seawater (16) yet abundant and highly expressed in enriched waters (17). Copiotrophs exhibiting chemotaxis may frequently outcompete oligotrophs that do not swim, and vice versa, yet we have a poor understanding and no predictive tools to determine the conditions under which either strategy is favored. To understand the ecological consequences of bacterial competition for DOM in the phycosphere, a link is needed between the microscale, where chemotaxis unfolds, and the ecosystem scale, where microbial activities integrate into the marine food web.

Here we examine the fate of diatom DOM using a hybrid approach that integrates high-resolution analysis of bacterial dynamics in phycospheres with a mathematical model that bridges microscale observations to ecosystem consequences. Experimentally, we created reproducible, controlled hotspots and attained the most detailed view of phycosphere hotspot dynamics to date. Mathematically, we used this observational data to model the consumption competition between a motile copiotrophic population and a nonmotile oligotrophic population, including an examination of the ocean conditions under which chemotaxis affects the consumption of DOM. This approach allowed us to predict the partitioning of DOM among and within bacterial populations and the effects of DOM consumption on bacterial population dynamics.

Results and Discussion

Natural Hotspots. Using time-lapse video microscopy, we repeatedly observed that the motile fraction of bacteria from an enriched coastal ocean community formed clusters around individual phytoplankton cells of different genera (Fig. 1 *A*–*C* and Movie S1) and other planktonic particles, including dead copepods and fecal pellets (Movie S2), all collected from the same samples as the bacteria. The clusters were often ephemeral, lasting from a few

Significance

Microscale interactions between bacteria and phytoplankton underpin ocean biogeochemistry and frequently involve bacterial chemotaxis to phytoplankton dissolved organic matter (DOM). Yet, it remains unclear how the effects of this interaction propagate to ecosystem scales. We address this gap through a hybrid approach where high-resolution observations of chemotaxis toward a diatom are directly used in a resource utilization model. We find that chemotactic bacteria consume most diatom DOM under resource-rich or bacteria-rich conditions, that DOM is partitioned among distinct populations based on diffusivity, and that consumption is skewed toward very few cells. Nonmotile oligotrophic bacteria dominate when productivity is low. Motile copiotrophs dominate during blooms. Ocean chemotaxis thus partitions resources spatially, by molecular size, and temporally through seasonal and episodic blooms.

Author contributions: S.S., V.I.F., J.G.M., and R.S. designed research; S.S. and V.I.F. performed research; S.S. and V.I.F. contributed new reagents/analytic tools; S.S. and V.I.F. analyzed data; and S.S., V.I.F., J.G.M., and R.S. wrote the paper.

The authors declare no conflict of interest.

This article is a PNAS Direct Submission.

[1]S.S. and V.I.F. contributed equally to this work.

[2]To whom correspondence should be addressed. Email: romanstocker@ethz.ch.

This article contains supporting information online at www.pnas.org/lookup/suppl/doi:10.1073/pnas.1512307113/-/DCSupplemental.

minutes to >1 h (Fig. 1 and Movie S2). For example, over 6 min a *Chaetoceros* diatom (Fig. 1 *A–C*, upper left) attracted a strong cluster of bacteria that was completely dissipated 3 min later. We interpret these accumulations as the chemotactic response of motile bacteria to the chemical gradients surrounding the phytoplankton cells and organic particles (10).

Community 16S rRNA gene analysis revealed that the enriched bacterial community used in experiments was dominated by *Vibrio* spp. and *Pseudoalteromonas* spp. (Fig. S1). These genera are frequently observed in coastal seawater, and the cultured isolates *Vibrio alginolyticus* and *Pseudoalteromonas haloplanktis* exhibit strong and rapid chemotaxis toward artificial microscale DOM plumes (18, 19). These genera also grow in response to short-term enrichments (20, 21), demonstrating their copiotrophic nature. Thus, enrichment with planktonic particles predictably stimulated growth of copiotrophic taxa, as occurs during natural resource enrichments such as phytoplankton blooms (4), and our analysis of phycosphere dynamics therefore focused on the responses of these copiotrophic genera.

Controlled Hotspots. To quantitatively characterize the spatiotemporal dynamics of a prototypical chemotactic cluster, we devised an approach to create microscale DOM hotspots on demand using the diatom *Chaetoceros affinis* (CCMP160), owing to its cosmopolitan distribution and frequent occurrence in natural samples (Fig. 1 *A–C*). We induced the lysis of individual *C. affinis* chains by 5- to 10-min exposure to fluorescent light (350 nm, 7 mW/mm^2) under the microscope, resulting in reproducible DOM pulses that mimic those naturally occurring in the ocean as a result of viral lysis (22) or "sloppy feeding" by zooplankton (23). Multiple cells in the diatom chains typically underwent lysis; whereas the diatom frustule usually remained intact, the plasma membrane collapsed (Fig. S2 and Movie S3).

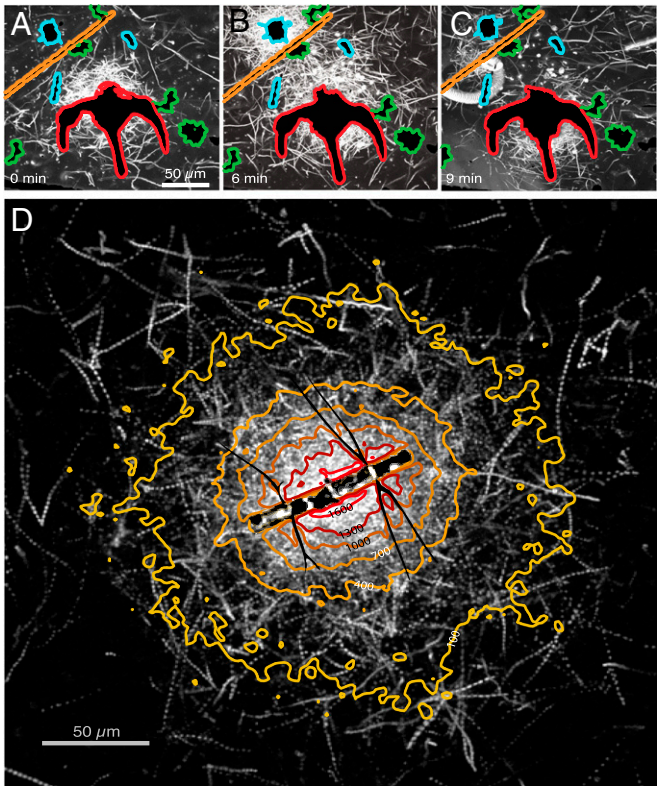

Fig. 1. Seawater bacteria respond to ephemeral DOM gradients from phytoplankton. (*A–C*) Swimming trajectories (white) of bacteria demonstrate ephemeral accumulations or "clusters" around natural phytoplankton including *Chaetoceros* sp. (aqua outline), *Ceratium* sp. (red), *Asterionella* sp. (green), and *Skeletonema* sp. (orange). The image at each time point is the maximum intensity projection from a movie (Movie S1). (*D*) Chemotactic cluster formation around the cultured diatom *C. affinis*. Contours show the enhancement of motile bacteria over background concentration during the 30 s immediately following cell lysis (Fig. S4). White tracks are bacterial trajectories over 2 s.

Upon diatom lysis, motile bacteria exhibited strong chemotaxis. A representative example (Fig. 1*D*) of six replicate experiments (Fig. S3) illustrates a bacterial cluster within the phycosphere, as determined from the quantification of individual bacterial positions with ∼1-μm resolution from time-lapse images acquired every 0.05 s (*SI Materials and Methods*). The enhancement of bacteria relative to the background concentration, $B(r,t)$, where r is the distance from the diatom center and t is time (*SI Materials and Methods*), shows an initial accumulation toward the diatom, followed by a sharp increase in intensity reaching greater than 1,000-fold above background (Fig. 1*D* and Fig. S4*B*). Quantitative metrics for cluster intensity and size (Fig. S4*C*) as well as coincident changes in diatom brightness (Fig. S4*A*) indicate that this accumulation occurred in response to more than one DOM release event, with the response to some individual releases reflected by brief contractions in the area of the bacterial cluster.

To determine the prototypical cluster response, and sidestep the complexity of multiple sequential lysis events, we repeated experiments on single, isolated *C. affinis* cells (Movie S4). The resulting bacterial distribution was nearly radially symmetric (Fig. 2*A*). The time course of the cell enhancement, $B(r,t)$, illustrates that the cluster formed within ∼1 min and dissipated after ∼10 min (Fig. 2 *B* and *C*), characteristics that were robustly observed across replicate single-cell lysis events ($n = 5$; Fig. S5) and consistent with previous studies (10, 24). Shortly after lysis, the cluster intensified substantially. An increase in bacterial concentration over background at distances of $r = 1.2$–1.8 mm from the diatom (Fig. S6; 3–6 min after lysis) indicates that detectable levels of released DOM reached these distances. Thus, for the purposes of modeling we define 2 mm as the radius of the phycosphere.

DOM Consumption Model. We used the observed bacterial enhancement, $B(r,t)$, in a mathematical model to quantify DOM consumption and predict the implications of hotspot exploitation on the competition for DOM between motile and nonmotile bacteria. Although DOM is often a complex mixture of molecules, we model it here for simplicity as a single compound, whose concentration $C(r,t)$ varies in space (r) and time (t) as a result of diffusion and consumption, that is,

$$\frac{\partial C}{\partial t} = D\nabla^2 C - [4\pi a_{\mathrm{NM}} D B_0 + 4\pi a_{\mathrm{M}} D B(r,t)\gamma B_0]\, C. \qquad [1]$$

The first term on the right-hand side represents molecular diffusion with diffusivity D. We identified the diffusivity of the effective chemoattractant as that which best corresponded to the observed bacterial response, recognizing that release of chemoattractant may not have been instantaneous (*SI Materials and Methods*). The two terms in square brackets express diffusion-limited DOM consumption by a population of nonmotile bacteria (25), having bulk concentration B_0 and individual-cell radius a_{NM}, and a population of motile bacteria having bulk concentration γB_0 and individual-cell radius a_{M}. Radii are equivalent-spherical-cell radii for ecologically relevant cell sizes (26) and are different between motile and nonmotile populations as a simple means to account for differences in uptake kinetics. The parameter γ represents the relative concentration of motile and nonmotile bacteria in bulk seawater. We chose a baseline value of ∼10% motility, typical of natural seawater communities, but explored the effect of this parameter over a broad range, representative of the variability observed in nature (14, 15, 27). Nonmotile bacteria maintain their uniform bulk concentration B_0 at all times, lacking the ability to behaviorally respond to the DOM. Thus, the model extends our observations by including a nonmotile population (*SI Materials and Methods*) and the quantification of the consumption by each population, obtained from

the model, is the basis for determining the outcome of the competition for the diatom's DOM.

Fate of Diatom-Derived DOM. When the bulk bacterial concentration is high, a large fraction of the DOM released by lysis is consumed locally within the phycosphere, mostly by motile cells. Assuming a 1:10 ratio of motile to nonmotile bacteria ($\gamma = 0.1$) and that motile bacteria are larger ($a_M = 0.5\ \mu m > a_{NM} = 0.2\ \mu m$), we used the model to compute the fraction of DOM consumed by all cells within a single phycosphere ($r < 2$ mm) and the partitioning of this consumption between motile and nonmotile bacteria (Fig. 3*A*). For $B_0 < 10^5$ cells per mL, consumption in the phycosphere is negligible and most DOM diffuses past the clustered bacteria and out of the phycosphere (Fig. 3*A*, *Inset*). Conversely, when $B_0 = 10^6$ cells per mL then 25% of the DOM is consumed within the phycosphere, and when $B_0 = 10^7$ cells per mL—as can occur during phytoplankton blooms (28)—this fraction increases to 92% (Fig. 3*A*, *Inset*). Phycosphere consumption is dominated in all cases (for $B_0 = 10^4$ to 10^8 cells per mL) by motile bacteria, which obtain greater than fivefold more DOM in the phycosphere than nonmotile bacteria (Fig. 3*A*).

DOM not consumed in the phycosphere diffuses into bulk seawater ($r > 2$ mm), where it becomes homogeneously distributed and consumed over time by homogeneously distributed motile and nonmotile bacteria. The sum of each population's consumption in the two regimes—the phycosphere and the bulk—determines the outcome of the competition, and when phycosphere consumption is negligible, then each population's consumption is determined solely by its uptake rate in the bulk, irrespective of behavior. Accounting for this (*SI Materials and Methods*), we find that motile bacteria consume 22–36% of released DOM at bulk bacterial concentrations typical of seawater ($B_0 = 10^5$ to 10^6 cells per mL), 50% at slightly elevated bulk concentrations ($B_0 = 2.2 \times 10^6$ cells per mL), and a striking 82% at high bulk concentrations ($B_0 = 10^7$ cells per mL) (Fig. S7).

An analysis of the resource competition equation (Eq. **1**) shows that DOM partitioning can be predicted for a broad range of different bulk bacterial concentrations B_0, cell sizes a_{NM} and a_M, and proportion of motile cells γ, using only two lumped parameters, $\Sigma = 4\pi D a_{NM} B_0$ and $\Gamma = \gamma a_M / a_{NM}$ (Fig. 3*B*). The nonmotile consumption strength parameter, Σ (an inverse timescale), represents the uptake rate of the population of nonmotile bacteria, whereas the consumption strength ratio, Γ (dimensionless), measures the uptake rate of the motile population ($4\pi D a_M \gamma B_0$) over that of the nonmotile population ($4\pi D a_{NM} B_0$), both computed assuming a uniform distribution of bacteria. For low consumption strengths ($\Sigma < \sim 10^{-5}\ s^{-1}$, $\Gamma < \sim 1$; Fig. 3*B*), the fraction of the DOM consumed overall by motile bacteria, F_{MOT}, is set by Γ alone, because consumption is negligible within the phycosphere and occurs almost entirely in the bulk (Fig. 3*A*). This "bulk limit" represents the traditional view of bacterial consumption in the ocean, in which microscale resource heterogeneity is not considered. For $\Sigma > \sim 10^{-4}\ s^{-1}$, consumption occurs primarily in the phycosphere and is dominated by the motile population for all but the smallest values of Γ. For example, we find that motile bacteria consume $F_{MOT} = 29\%$ of released DOM in typical coastal seawater conditions (Fig. 3*B*, white circle; $\Sigma = 4.0 \times 10^{-5}\ s^{-1}$, $\Gamma = 0.25$; i.e., $B_0 = 5 \times 10^5$ cells per mL, $a_M = 0.5\ \mu m$, $a_{NM} = 0.2\ \mu m$, $\gamma = 0.1$). This value jumps to $F_{MOT} = 93\%$ in typical diatom bloom conditions (Fig. 3*B*, white triangle; $\Sigma = 7.9 \times 10^{-4}\ s^{-1}$, $\Gamma = 0.5$; i.e., $B_0 = 10^7$ cells per mL, $a_M = 1.0\ \mu m$, $a_{NM} = 0.2\ \mu m$, $\gamma = 0.1$). These results reveal that under typical coastal conditions the partitioning of DOM among bacterial populations is largely unaffected by motility, and this is consistent with the variable and often low prevalence of swimming cells observed in natural waters (14, 27). In contrast, in hotspot-rich conditions such as blooms, chemotaxis can play a disproportionate role in the fate of DOM from phytoplankton, even when the fraction of motile bacteria is small.

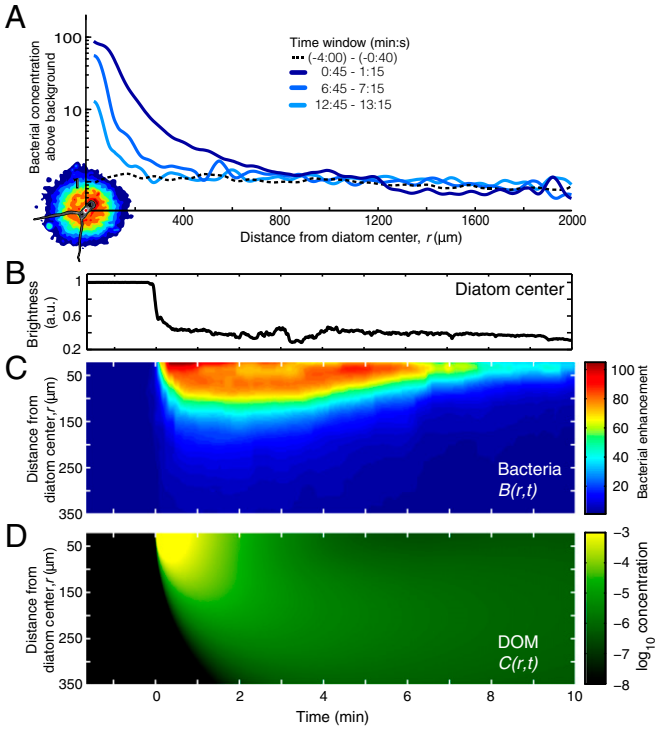

Fig. 2. Chemotactic accumulation in the phycosphere lasts ~10 min and extends ~2 mm from the diatom. All panels (*A*–*D*) show results for a prototypical radially symmetric cluster in response to lysis of a single *C. affinis* diatom. (*A*) Bacterial concentration above background as a function of distance from the diatom center, *r*, for three 30-s time windows after lysis. The prelysis background is also shown. An image of the lysed diatom (bottom left) shows relative bacterial concentration (color contours) at peak accumulation ($t = 1$ min), with the same scale as the *x* axis. (*B*) Brightness of the diatom center (in arbitrary units) showing the moment at which lysis occurred, $t = 0$. (*C*) Bacterial enhancement relative to the background concentration, $B(r,t)$. (*D*) Relative concentration of the effective chemoattractant as a function of distance and time, $C(r,t)$, determined from a mathematical simulation.

A Bountiful Yet Risky Phycosphere? By bringing bacteria in close proximity to the diatom and each other, cluster formation can influence the exchange of substances beyond the chemoattractant(s). These can include other molecules from the diatom but also biological entities originating from the accumulated bacteria themselves, for example signaling molecules, phages, or vesicles (29), the release of which can be approximated as originating from the diatom lysis. We quantified the potential for exchange enhancement for different substances by running the model for different values of the diffusivity *D* and the observed cluster dynamics quantified by $B(r,t)$. Molecules with intermediate diffusivities ($D = 3.2 \times 10^{-12}$ to $3.2 \times 10^{-9}\ m^2 s^{-1}$), characteristic of many that can be released during diatom lysis, are consumed predominately (>50%) by motile cells (Fig. 3*C*). For example, consumption of proteins similar in size to GFP [$D = 9 \times 10^{-11}\ m^2 s^{-1}$ (30)] will be strongly dominated by motile bacteria (83%), which is consequential because phytoplankton are composed of >50% protein (31). In contrast, molecules with very high diffusivity ($D > 10^{-8}\ m^2 s^{-1}$) escape from the phycosphere before being consumed. Meanwhile, substances with very low diffusivity ($D < 10^{-12}\ m^2 s^{-1}$) disperse much more slowly than the ~10-min duration of a cluster, hence they are not preferentially captured by motile bacteria. A consequence of this last result is that, although clustering allows motile bacteria to dominate DOM consumption in the phycosphere, it does not enhance their exposure to low-diffusivity entities that may be present in high concentrations in the cluster, such as phages (Fig. 3*C*). Based on this prediction, we speculate that motile bacteria take advantage of DOM hotspots while minimizing the risk of "dangerous exchanges" within them. Moreover, enzyme activity among clustered bacteria may degrade low-diffusivity DOM to

ECOLOGY

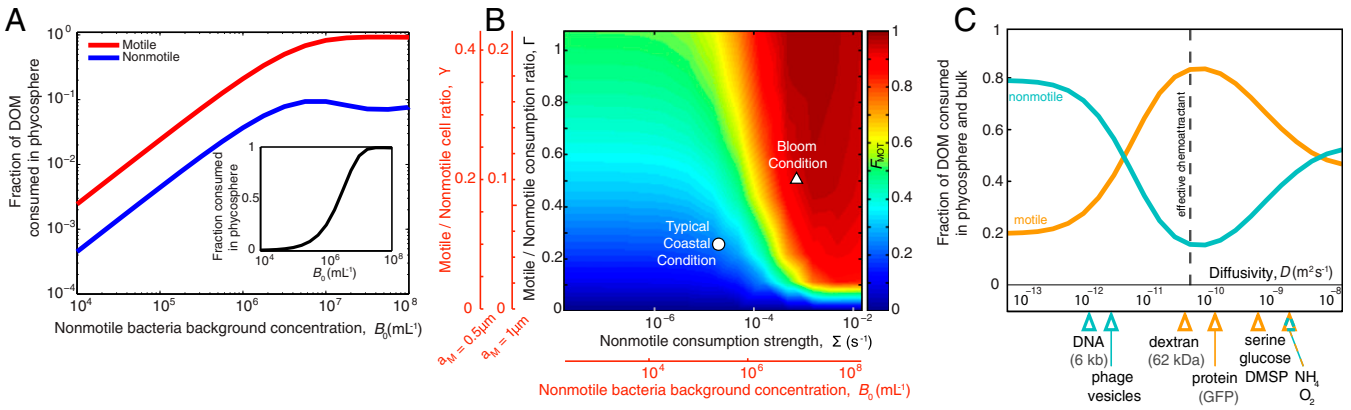

Fig. 3. Motile bacteria often dominate consumption of DOM released from phycospheres. (*A*) Fraction of DOM released in a lysis that is consumed within the phycosphere ($r < 2$ mm from the diatom center), and within the duration of accumulation (10 min), by motile (red) and nonmotile (blue) bacteria, as a function of the background concentration of nonmotile bacteria, B_0. (*Inset*) Fraction of DOM consumed in the phycosphere by both populations together. (*B*) Fraction of DOM consumed by motile bacteria (F_{MOT}; color bar), calculated for a broad range of motile to nonmotile cell number ratios γ, background bacterial concentrations B_0, and cell sizes a_M and a_{NM}. Red axes show F_{MOT} for two selected values of motile cell size, a_M, with nonmotile cell size fixed at $a_{NM} = 0.2$ μm. Black axes shows F_{MOT} as a function of the nonmotile consumption strength, $\Sigma = 4\pi\, a_{NM}\, D\, B_0$,[$s^{-1}$], and the dimensionless consumption ratio, $\Gamma = a_M/a_{NM}\, \gamma$. Two scenarios are identified by the white symbols (discussed in the main text). (*C*) Fraction of DOM consumed overall by motile (orange) and nonmotile (cyan) bacteria as a function of the diffusivity D (for $B_0 = 10^7$ cells per mL). The diffusivity of the effective chemoattractant in the experiments is indicated by the dashed line ($D = 3 \times 10^{-11}$ m^2/s). Values of D for some biomolecules are indicated by arrowheads and color-matched to the population that dominates consumption of that molecule. For *A*, *B*, and *D*: $\gamma = 0.1$, $a_M = 0.5$ μm, and $a_{NM} = 0.2$ μm.

create high-diffusivity hydrolysates (32, 33), further enhancing uptake by chemotactic cells in the phycosphere.

From a Single Phycosphere to the Phycoscape. The importance of phycospheres for bacterial populations will depend on consumption by individual bacteria over multiple phycosphere encounters in the ocean resource landscape. To scale up predictions of consumption from a single phycosphere to this "phycoscape," we consider an ocean in which diatom lysis hotspots are the sole carbon source for two competing bacterial populations under three scenarios: typical coastal conditions, a phytoplankton bloom, and a bloom collapse, corresponding to 34, 312, and 912 lyses per mL per d, respectively (*SI Materials and Methods*). Assuming that lysis events are uncorrelated and bacteria never experience overlapping phycospheres, individual bacteria encounter phycospheres as a Poisson process with average encounter rates of 1 per d, 10 per d, and 31 per d, respectively (Fig. S8 and *SI Materials and Methods*). In this model ocean, bacteria consume DOM both within phycospheres and in the bulk, where the bulk, steady-state DOM concentration is determined by the amount of DOM escaping from phycospheres and by the concentration of bacteria (Fig. 3*A*, *Inset*).

At the phycoscape level, there is a distinct transition in bacterial growth between bulk-dominated and phycosphere-dominated regimes (Fig. 4 and Fig. S9), mirroring the behavior observed in the partitioning of DOM from a single diatom. At low bacterial concentrations ($B_0 < 10^6$ cells per mL), elevated levels of carbon in the bulk drive growth, giving an advantage to the nonmotile population. At high bacterial concentrations ($B_0 > 10^7$ cells per mL), carbon consumption occurs primarily within phycospheres and little leaks into the bulk, which strongly favors motile bacteria. The point of transition between the two regimes depends on the ratio γ of motile to nonmotile bacteria: For a 1:10 ratio, the transition occurs at $B_0 = 5 \times 10^6$ cells per mL (Fig. 4), whereas for a 1:1 ratio it occurs at $B_0 = 0.8 \times 10^6$ cells per mL. In the typical coastal scenario considered, carbon from lysis events supports growth of less than one new motile cell per day, insufficient to sustain the population under a characteristic assemblage turnover time of 1 d (34). In contrast, in the phytoplankton bloom or bloom collapse scenarios, growth benefits for both bacterial populations become substantial as cells encounter more lysis events (Fig. 4), and a higher percent of cells reproduce (Fig. S10 *A*–*C*). Even while both populations grow better, motility yields a >300% growth advantage in the bloom collapse scenario when $B_0 = 10^7$ cells per mL, a difference that remains conspicuous even after accounting for the cost of swimming (Fig. S11 and *SI Materials and Methods*).

The increased role of motile copiotrophs in DOM consumption under increased cell concentration, B_0 (Fig. 4), provides a mechanism for the initiation of bacterial succession in phytoplankton blooms. This is revealed by a simulation of the first several days of a bloom, starting from bacterial abundances typical of coastal conditions ($B_0 = 0.5 \times 10^6$ bacteria per mL, ref. 35; $\gamma = 0.1$) and accounting for losses due to viral infection and protistan grazing (*SI Materials and Methods*). The simulation predicts a turnover in biomass from nonmotile oligotrophs to motile copiotrophs (Fig. 5*A*): Populations increase after the bloom begins, heightening the competition for DOM and thus the importance of phycosphere consumption, and triggering the dominance of bacterial biomass by motile bacteria after ~4 d (Fig. 5*A*). In this scenario, nonmotile bacteria still dominate numerically ($\gamma_{MAX} = 0.25$), but the larger cell size of motile bacteria and their dominance of phycosphere consumption triggers the biomass "inversion." This inversion will amplify during a bloom collapse, when phycosphere encounters increase even further.

During a bloom, when consumption is phycosphere-driven, the statistical nature of phycosphere encounters by individual bacteria results in a strong skew in uptake among motile bacteria as well as among nonmotile bacteria. Quantifying single-cell uptake in these conditions (*SI Materials and Methods*) revealed that a few "superconsumer" cells, those that happen to encounter multiple phycospheres and/or to be in a favorable location within a phycosphere, consume vastly more DOM than the average cell. For example, during a single lysis event (for $B_0 = 10^7$ cells per mL) the top 1% of motile cells consume enough DOM to each produce >30 new cells (Fig. S12). Scaling this up to the phytoplankton bloom scenario, the top 1% of motile cells account for 40% of the population's total DOM consumption (Fig. 5*B* and Fig. S10*E*). This reveals that population reproduction may be largely driven by a small number of superconsumer cells. Consumption inequality during a bloom is even greater among nonmotile bacteria, where the 1% superconsumers account for 60% of the population's total consumption (for $B_0 = 10^7$ cells per mL; Fig. 5*B* and Fig. S10 *E* and *F*), owing to the absence of cell redistribution within the phycosphere.

Impacts on the Microbial Ocean. DOM in the surface ocean often becomes available to microbes as microscale hotspots, in the form of organic particles (33), leakage or lysis of phytoplankton, and microscale filaments originating from the turbulent stirring of

larger DOM patches (36). However, consumption of DOM is not always correspondingly heterogeneous: Consumption can occur within the hotspots but also in the bulk. Our hybrid observation-modeling framework enables one to predict the conditions under which bacterial DOM consumption is bulk-dominated versus hotspot-dominated (Fig. 3*B*). We find that consumption among free-living bacteria is bulk-dominated under typical coastal ocean conditions, when most DOM released as microscale patches diffuses past bacteria that have accumulated by chemotaxis into bulk seawater, where consumption is dominated by nonmotile oligotrophs. In contrast, consumption becomes hotspot-dominated in phytoplankton blooms and bloom collapse conditions, when bacterial concentrations are high, cells are large, and/or the percentage of motile cells is elevated (Fig. 3*B*).

When the environment shifts toward a higher frequency of hotspots, the growth of motile cells creates positive feedback by hastening the development of hotspot-dominated conditions, which in turn skews consumption toward motile cells. In addition to chemotaxis, the growth of motile cells will be strengthened by other copiotrophic adaptations, including diversified membrane transporters and higher ribosome content (2), as well as multiphasic uptake kinetics (37). Chemotaxis then enables copiotrophs to deploy these adaptations with great effectiveness within hotspots, even when phycospheres are distorted by fluid flow (*SI Discussion*), potentially further increasing the per capita utilization of DOM compared with that found in our analysis.

The accumulation of copiotrophs in the phycosphere marks the initial stage in a continuum of events following a phytoplankton's lysis. Chemotaxis may favor and precede attachment of some bacteria to the diatom surface, enabling colonization of nascent phytodetrital particles. Attached bacteria that produce hydrolytic enzymes can degrade particulate organic matter embedded in the diatom (38), releasing additional DOM. Because the timescale of attachment can be much greater than the initial ~10-min-long response to lysis, the enzymatic activity of attached cells may create long-term gradients, prolonging the effect of the phycosphere on bacterial competition. Our observations demonstrate that clusters are mostly dissipated after 10 min (Fig. 2), suggesting that DOM gradients become too weak to trigger substantial accumulation and that DOM exuded from phytodetritus on longer timescales should partition primarily to nonmotile oligotrophs. In contrast, attached copiotrophs will have prolonged individual benefits.

Growth of motile cells in hotspot-dominated conditions will modify the composition of bacterial assemblages by leading to greater prevalence of copiotrophic taxa. Despite observational evidence that major perturbations to the DOM environment trigger succession among bacteria, with a dominance of copiotrophic groups (4), no quantitative framework has been available for these observations. Our analysis provides such a framework, for the simplified case of two bacterial populations, for which it predicts both the trends and the turning points for bacterial succession, in particular revealing that the initial phase of succession is driven by competition for DOM that becomes increasingly localized (Fig. 5*A*). Importantly, the model predicts the dynamics of the relative concentration of motile and nonmotile bacteria (γ), a parameter analogous to the relative representation of motility and chemotaxis genes in metaomic datasets (17, 39). The model therefore provides context for interpreting relative gene data and potentially converting such data post hoc to an empirical ratio for motile to nonmotile cells.

For motile bacteria and nonmotile bacteria, the effect of "being in the right place at the right time" has large consequences for individual uptake when DOM appears as ephemeral hotspots. Uptake distributions are strongly skewed within a population (Fig. S10) and a small number of superconsumer individuals, belonging to the long tail of the per-cell consumption curve, are responsible for most of the total population uptake. This hetereogeneity is commonly averaged out in bulk sampling approaches and seldom appreciated in marine microbial ecology. Intriguingly, long-tailed distribution curves also characterize single-cell activity rates in coastal seawater (40, 41), suggesting a relationship between the uptake heterogeneity resulting from hotspots and skewed rates in standing bacterial stocks, which may extend to the level of individual phylotypes.

The concept of the phycosphere has evolved from theory (7–9, 12) to observation (10, 11, 13) and, with this study, to controlled generation and high-resolution quantification, indispensable steps to permit up-scaling its consequences for consumption and growth among bacterial populations. The hybrid approach

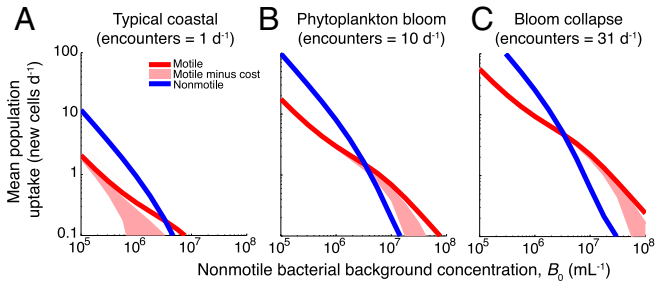

Fig. 4. Bacterial growth in a seascape of lysing diatom, illustrating the advantage of motility at high lysis encounter rates and high bacterial concentrations. Three characteristic environmental conditions are shown: typical coastal seawater, a phytoplankton bloom, and a bloom collapse. (*A*–*C*) Mean population uptake for motile and nonmotile cells, expressed in new cell carbon equivalents per day, as a function of the background concentration of nonmotile bacteria, B_0. For all panels, the motile:nonmotile cell number ratio was 1:10 (γ = 0.1). Shaded pink areas indicate motile population benefits after subtracting costs for swimming, for a range of assumed swimming velocities and efficiencies (*SI Materials and Methods*).

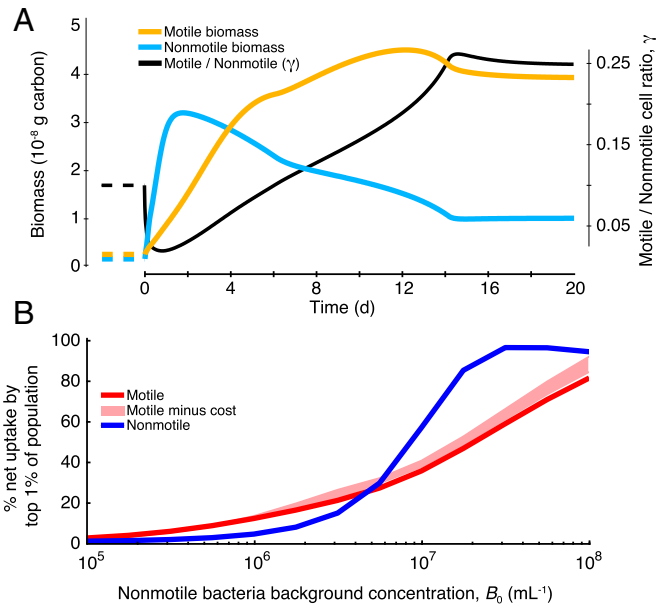

Fig. 5. Bacterial growth during a phytoplankton bloom, illustrating the effects of phycospheres on the initiation of succession among populations of bacteria. (*A*) Biomass of motile (yellow) and nonmotile (cyan) cells and motile:nonmotile cell number ratio γ (black). The bloom was simulated by exposing both populations over several days to a constant lysis encounter rate of 10 per d. Before bloom initiation (dashed lines), conditions for the bacteria populations were set at γ = 0.1, nonmotile background bacterial concentration $B_0 = 5 \times 10^5$ cells per mL, and cell sizes a_M = 0.5 μm and a_{NM} = 0.2 μm. (*B*) Contribution by the top 1% of cells to the overall population consumption of DOM by each population. For *B*, results are for 1-d exposure to a bloom where B_0 was fixed (accordingly) and γ = 0.1, and shaded pink areas indicate motile population benefits after subtracting costs for swimming (Fig. 4).

ECOLOGY

introduced here opens the door to its application for other studies of microscale patch dynamics and provides a blueprint for studying bacterial competition in heterogeneous environments. Different resource hotspots—including diverse groups of phytoplankton, particles, and oil droplets, as well as different release rates spanning from slow leakage to sudden lysis—will result in different microscale resource seascapes and thus different outcomes of the competition. The extension of both the laboratory approach and the modeling framework to the spectrum of microscale hotspots making up the ocean's chemical seascape will provide a fertile avenue toward a deeper understanding of the foraging ecology of microorganisms and their effects on microbial competition, genetic diversity, and ocean biogeochemistry.

Materials and Methods

Experimental Conditions for Diatom Lysis and Chemotactic Bacterial Response. We developed an approach to stimulate chemotactic cluster formation by inducing the lysis of individual chains or cells of the diatom *C. affinis*. In a mixture of enriched bacteria and diatom culture, a diatom was centered within the microscope's field of view and the iris constricted to shine fluorescent light only on the diatom and its immediate vicinity, over a circular area of ~10-μm radius. To initiate diatom lysis, blue fluorescence light (350 nm excitation, 7 kW/m^2) was applied for 5–10 min while maintaining continual broad-spectrum light-emitting diode (LED) white-light illumination (~200 μmol m^{-2} s^{-1}). This procedure stimulated diatom plasmolysis, which was followed by chemotactic accumulation of motile bacteria 3–4 min after the fluorescence light was turned off. Image capture via video microscopy occurred during light exposure and through the chemotactic clustering response for up to 60 min.

Other Methods. Seawater sampling, diatom maintenance, microscopy, image analysis, and mathematical modeling are described in Supporting Information.

ACKNOWLEDGMENTS. We thank Antonio Platero for laboratory assistance and Kay Bidle, Filippo Menolascina, Jennifer Nguyen, Michael Sieracki, and Assaf Vardi for discussions. This work was supported by a National Science Foundation Ocean Sciences Postdoctoral Fellowship (to S.S.), an Australian Research Council grant (to J.G.M.), and Gordon and Betty Moore Marine Microbial Initiative Investigator Award GBMF 3783 (to R.S.).

1. Koch AL (2001) Oligotrophs versus copiotrophs. *BioEssays* 23(7):657–661.
2. Lauro FM, et al. (2009) The genomic basis of trophic strategy in marine bacteria. *Proc Natl Acad Sci USA* 106(37):15527–15533.
3. Mayali X, Weber PK, Mabery S, Pett-Ridge J (2014) Phylogenetic patterns in the microbial response to resource availability: Amino acid incorporation in San Francisco Bay. *PLoS One* 9(4):e95842.
4. Teeling H, et al. (2012) Substrate-controlled succession of marine bacterioplankton populations induced by a phytoplankton bloom. *Science* 336(6081):608–611.
5. Pedler BE, Aluwihare LI, Azam F (2014) Single bacterial strain capable of significant contribution to carbon cycling in the surface ocean. *Proc Natl Acad Sci USA* 111(20):7202–7207.
6. Stocker R (2012) Marine microbes see a sea of gradients. *Science* 338(6107):628–633.
7. Mitchell JG, Okubo A, Fuhrman JA (1985) Microzone surrounding phytoplankton form the basis for a stratified marine microbial ecosystem. *Nature* 316(6023):58–59.
8. Bell W, Mitchell R (1972) Chemotactic and growth responses of marine bacteria to algal extracellular products. *Biol Bull* 143(2):265–277.
9. Blackburn N, Azam F, Hagstrom A (1997) Spatially explicit simulations of a microbial food web. *Limnol Oceanogr* 42(4):613–622.
10. Blackburn N, Fenchel T, Mitchell J (1998) Microscale nutrient patches in planktonic habitats shown by chemotactic bacteria. *Science* 282(5397):2254–2256.
11. Blackburn N, Fenchel T (1999) Influence of bacteria, diffusion and sheer on micro-scale nutrient patches, and implications for bacterial chemotaxis. *Mar Ecol Prog Ser* 189:1–7.
12. Azam F, Ammerman JW (1984) Cycling of organic matter by bacterioplankton in pelagic marine ecosystems: microenvironmental considerations. *Flows of Energy and Materials in Marine Ecosystems*, ed Fasham MJR (Plenum, New York), pp 345–360.
13. Fenchel T (2002) Microbial behavior in a heterogeneous world. *Science* 296(5570): 1068–1071.
14. Grossart HP, Riemann L, Azam F (2001) Bacterial motility in the sea and its ecological implications. *Aquat Microb Ecol* 25(3):247–258.
15. Mitchell JG, et al. (1995) Long lag times and high velocities in the motility of natural assemblages of marine bacteria. *Appl Environ Microbiol* 61(3):877–882.
16. Yooseph S, et al. (2007) The Sorcerer II Global Ocean Sampling expedition: Expanding the universe of protein families. *PLoS Biol* 5(3):e16.
17. McCarren J, et al. (2010) Microbial community transcriptomes reveal microbes and metabolic pathways associated with dissolved organic matter turnover in the sea. *Proc Natl Acad Sci USA* 107(38):16420–16427.
18. Seymour JR, Simó R, Ahmed T, Stocker R (2010) Chemoattraction to dimethylsulfoniopropionate throughout the marine microbial food web. *Science* 329(5989):342–345.
19. Stocker R, Seymour JR, Samadani A, Hunt DE, Polz MF (2008) Rapid chemotactic response enables marine bacteria to exploit ephemeral microscale nutrient patches. *Proc Natl Acad Sci USA* 105(11):4209–4214.
20. Mitchell JG, Pearson L, Dillon S, Kantalis K (1995) Natural assemblages of marine bacteria exhibiting high-speed motility and large accelerations. *Appl Environ Microbiol* 61(12): 4436–4440.
21. Takemura AF, Chien DM, Polz MF (2014) Associations and dynamics of Vibrionaceae in the environment, from the genus to the population level. *Front Microbiol* 5:38.
22. Gobler CJ, Hutchins DA, Fisher NS, Cosper EM, Sanudo-Wilhelmy SA (1997) Release and bioavailability of C, N, P, Se, and Fe following viral lysis of a marine chrysophyte. *Limnol Oceanogr* 42(7):1492–1504.
23. Strom SL, Benner R, Ziegler S, Dagg MJ (1997) Planktonic grazers are a potentially important source of marine dissolved organic carbon. *Limnol Oceanogr* 42(6):1364–1374.
24. Jackson GA (2012) Seascapes: The world of aquatic organisms as determined by their particulate natures. *J Exp Biol* 215:1017–1030.
25. Kiorboe T (2008) Random walk and diffusion. *A Mechanistic Approach to Plankton Ecology* (Princeton Univ Press, Princeton), pp 10–34.
26. Mitchell JG (1991) The influence of cell size on marine bacterial motility and energetics. *Microb Ecol* 22(1):227–238.
27. Fenchel T (2001) Eppur si muove: Many water column bacteria are motile. *Aquat Microb Ecol* 24(2):197–201.
28. Li WKW (1998) Annual average abundance of heterotrophic bacteria and Synechococcus in surface ocean waters. *Limnol Oceanogr* 43(7):1746–1753.
29. Biller SJ, et al. (2014) Bacterial vesicles in marine ecosystems. *Science* 343(6167):183–186.
30. Milo R, Jorgensen P, Moran U, Weber G, Springer M (2010) BioNumbers–the database of key numbers in molecular and cell biology. *Nucleic Acids Res* 38(Database issue):D750–D753.
31. Sarmiento JL, Gruber N (2006) Organic matter production. *Ocean Biogeochemical Dynamics* (Princeton Univ Press, Princeton), pp 116–117.
32. Bidle K (2010) Phytoplankton-bacteria interactions: Ectohydrolytic enzymes and their influence on biogeochemical cycling. *ASLO Web Lectures* 2(1):1–50.
33. Azam F, Malfatti F (2007) Microbial structuring of marine ecosystems. *Nat Rev Microbiol* 5(10):782–791.
34. Fuhrman JA, Noble RT (1995) Viruses and protists cause similar bacterial mortality in coastal seawater. *Limnol Oceanogr* 40(7):1236–1242.
35. Whitman WB, Coleman DC, Wiebe WJ (1998) Prokaryotes: The unseen majority. *Proc Natl Acad Sci USA* 95(12):6578–6583.
36. Taylor JR, Stocker R (2012) Trade-offs of chemotactic foraging in turbulent water. *Science* 338(6107):675–679.
37. Azam F, Hodson RE (1981) Multiphasic kinetics for D-glucose uptake by assemblages of natural marine-bacteria. *Mar Ecol Prog Ser* 6(2):213–222.
38. Bidle KD, Azam F (2001) Bacterial control of silicon regeneration from diatom detritus: Significance of bacterial ectohydrolases and species identity. *Limnol Oceanogr* 46(7):1606–1623.
39. Jeffries TC, et al. (2012) Increases in the abundance of microbial genes encoding halotolerance and photosynthesis along a sediment salinity gradient. *Biogeosci* 9(2):815–825.
40. Samo TJ, Smriga S, Malfatti F, Sherwood BP, Azam F (2014) Broad distribution and high proportion of protein synthesis active marine bacteria revealed by click chemistry at the single cell level. *Front Mar Sci* 1:48.
41. del Giorgio P, Gasol J (2008) Physiological structure and single-cell activity in marine bacterioplankton. *Microbial Ecology of the Oceans*, ed Kirchman DL (Wiley, Hoboken, NJ), 2nd Ed, pp 243–298.
42. Luchsinger RH, Bergersen B, Mitchell JG (1999) Bacterial swimming strategies and turbulence. *Biophys J* 77(5):2377–2386.
43. Confer DR, Logan BE (1991) Increased bacterial uptake of macromolecular substrates with fluid shear. *Appl Environ Microbiol* 57(11):3093–3100.
44. Rusconi R, Guasto JS, Stocker R (2014) Bacterial transport suppressed by fluid shear. *Nat Phys* 10(3):212–217.
45. Kiorboe T, Jackson GA (2001) Marine snow, organic solute plumes, and optimal chemosensory behavior of bacteria. *Limnol Oceanogr* 46(6):1309–1318.
46. Caporaso JG, et al. (2011) Global patterns of 16S rRNA diversity at a depth of millions of sequences per sample. *Proc Natl Acad Sci USA* 108(Suppl 1):4516–4522.
47. Crank J (1975) *The Mathematics of Diffusion* (Clarendon, Oxford), 2nd Ed.